Peruvian Stratus Clouds and the Tropical Pacific Circulation: A Coupled Ocean–Atmosphere GCM Study

CHUNG-CHUN MA, CARLOS R. MECHOSO, ANDREW W. ROBERTSON, AND AKIO ARAKAWA

Department of Atmospheric Sciences, University of California, Los Angeles, Los Angeles, California

(Manuscript received 11 August 1995, in final form 30 January 1996)

ABSTRACT

Extensive and persistent stratus cloud decks are prominent climatic features off the Peruvian coast. They are believed to play a key role in the coupled atmosphere–ocean processes that determine the sea surface temperature (SST) throughout the eastern tropical Pacific. This notion is examined and further developed using a coupled ocean–atmosphere general circulation model (GCM): a control simulation, in which the simulated amount of Peruvian stratus clouds is unrealistically low, is compared with an experiment in which a stratus cloud deck is *prescribed* to persistently cover the ocean off the Peruvian coast.

Beneath the prescribed cloud deck SSTs are reduced by up to 5 K, as expected from decreased solar radiation reaching the surface. In addition, there is significant cooling over much of the eastern tropical Pacific south of the equator, and even along the equator well into the central Pacific. The prescribed stratus deck largely alleviates the coupled GCM's warm bias in SST in the southeastern Pacific, which is common to most contemporary coupled GCMs, and produces a distribution of SST with more realistic interhemispheric asymmetries.

Examination of differences between SST evolutions in the enhanced stratus experiment and the control simulation reveals that the remote ocean cooling is not due to a single mechanism. The cooling immediately to the west and north of the region with the prescribed stratus deck is primarily associated with increased evaporation as the southeast trades strengthen. The cooling along the equator in the central Pacific is mainly due to increased oceanic cold advection.

The results of this study suggest that the Peruvian stratus clouds are important in modulating the circulation of the tropical Pacific. The "double ITCZ" syndrome of the coupled GCM, however, does not appear to be solely due to underpredicted stratus cloud cover and requires consideration of other processes in the coupled GCM.

1. Introduction

The large asymmetry of sea surface temperature (SST) about the equator is one of the most striking features of the climate over the eastern tropical Pacific. In this region SSTs are higher to the north and lower to the south throughout the seasonal cycle. The corresponding SST distribution obtained in simulations by almost all contemporary coupled general circulation models (GCMs) does not exhibit a comparable asymmetry. Without exception, all 11 coupled GCMs examined in Mechoso et al. (1995) produce an overly symmetric SST distribution in the eastern equatorial Pacific, with warm biases extending thousands of kilometers off the coast of Peru in a zonal band just south of the equator. Consider, for example, the difference between the annual mean SST in the tropical Pacific simulated by the UCLA coupled GCM and the observational estimates by Shea et al. (1990) as shown in Fig. 1. In spite of a systematic cold bias over most of the domain, there are conspicuous warm biases off the coasts of Peru and California. The warm bias off the coast of Peru, in particular, extends westward well into the central Pacific.

The systematic SST errors in the eastern tropical Pacific go together with serious deficiencies in the simulated atmospheric circulation. In many of the coupled GCMs reviewed by Mechoso et al. (1995), there is strong surface convergence over the anomalously warm waters just south of the equator, especially during the local summer; such convergence does not have an observational counterpart. The seasonal cycle simulated by these models includes either a migration of the intertropical convergence zone (ITCZ) across the equator or a double ITCZ straddling the equator, depending on the model. These deficiencies of coupled GCMs are of particular concern for simulations and predictions of El Niño–Southern Oscillation (ENSO), which is believed to be strongly linked to the seasonal cycle (see, e.g., Jin et al. 1994).

The ultimate source of meridional asymmetry about the equator of the circulation in the eastern Pacific is the interhemispheric asymmetries in the distribution of continents and oceans (e.g., Philander et al. 1996; manuscript submitted to *Nature*). The nearly parallel

Corresponding author address: Dr. Chung-Chun Ma, Department of Atmospheric Sciences, University of California, Los Angeles, 405 Hilgard Avenue, Los Angeles, CA 90095.

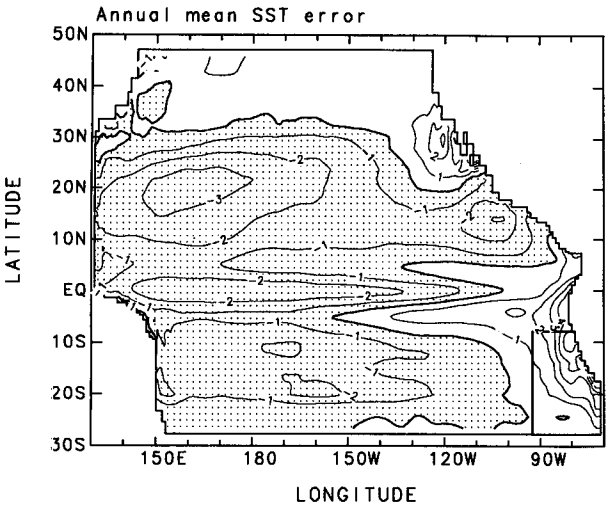

FIG. 1. Errors in annual mean climatological SST simulated by the UCLA coupled GCM. Contour interval is 1 K; regions with negative values are stippled.

alignment of the coast of Peru with the southeast trades favors coastal upwelling of cold subsurface water to the surface. In addition, the Peruvian coast lies beneath the descending branch of the Hadley–Walker circulation. The large static stabilities associated with cold SSTs and atmospheric subsidence result in extensive marine stratus cloud decks with areal coverages of 40%–70% on average. The seasonal peak is in October when the static stability—largely determined off Peru by the seasonal minimum in SST—is highest (Klein and Hartmann 1993). Through their high albedo, these stratus decks have a significant cooling effect on the underlying ocean. This cooling is only partially offset by the downward infrared emission from the clouds.

Figure 2 shows the annual mean stratus incidence in the UCLA coupled GCM and in its atmospheric component (AGCM) when observed SSTs are prescribed. Although a parameterization of stratus cloud is included in the model (following Suarez et al. 1983), both the coupled GCM and even the uncoupled AGCM fail to capture the high incidence of marine stratus characteristic of the coast of Peru. In the uncoupled AGCM, the net surface heat flux into the ocean is overestimated in this region. This deficiency is consistent with the warm SST bias in the coupled GCM (Fig. 1). In other coupled GCMs that exhibit similar systematic SST errors, the atmospheric component also tends to underestimate the stratus cloud in this region (Giese and Carton 1994; Stockdale et al. 1994; Philander et al. 1996a).

It should be kept in mind that coupled feedbacks between the atmosphere and ocean can play an important role in determining the characteristics of the circulation. Bjerknes (1969) pointed out a feedback between the zonal wind stress and the SST along the equator: Higher SST in the western Pacific, together with lower SST in the eastern Pacific, sets up a zonal surface pressure gradient in the atmosphere that drives a westward wind. The westward wind stress induces upwelling in the ocean at the equator. Because the thermocline is shallower in the east, this upwelling tends to cool the SST in the east more than that in the west, thus enhancing the SST gradient that sets up the atmospheric circulation in the first place. Dijkstra and Neelin (1995) have recently shown how similar feedbacks in an idealized model can greatly affect the strength and shape of the cold tongue in the zonal direction. In the meridional direction, Xie and Philander (1994) and Xie (1994) have demonstrated, using simple and hybrid models, respectively, how evaporation–wind feedback can produce an ITCZ asymmetric about the equator (e.g., to the north) even under boundary conditions that are symmetric.

The aim of this paper is to examine the role played by Peruvian stratus in the coupled atmosphere–ocean processes that determine the climate of the tropical Pa-

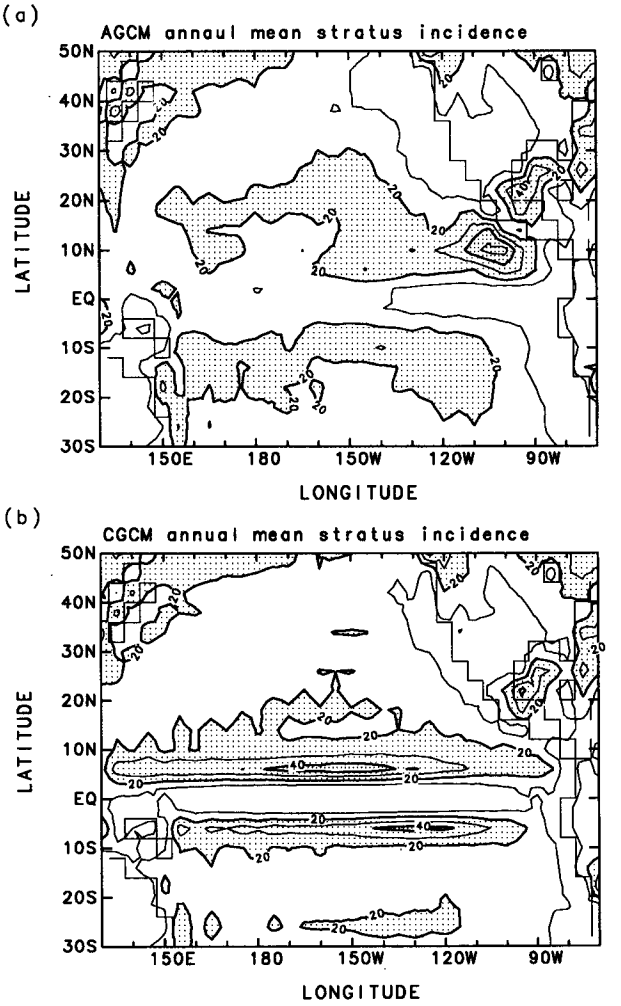

FIG. 2. Climatological annual mean stratus cloud incidence (percent) for (a) the uncoupled AGCM and (b) the coupled GCM. Contour interval is 10%; regions with values larger than 20% are stippled.

cific. Our approach is to examine the sensitivity of the climate simulated with a coupled GCM to the amount of stratus clouds off the Peruvian coast. Specifically, we perform an idealized experiment in which the stratus clouds predicted by the model in this region are artificially altered to provide persistent and high coverage. The results are compared with a control simulation that underestimates the Peruvian stratus. Although the underestimation of stratus clouds in other areas—such as the equatorial eastern Pacific and the region off California—may also have a strong influence on the tropical Pacific climate, in this paper we concentrate on the Peruvian stratus so that its effect can be better isolated.

We start in section 2 by describing the coupled GCM and the experimental setup and providing details on the model's parameterization of stratus clouds and their radiative effects. Sections 3 compares the climate and seasonal cycle of the two integrations. In section 4 we concentrate on the initial adjustments to study the physical processes involved. The implications of the results are discussed in section 5.

2. Model and experimental setup

The coupled GCM used in this study consists of the UCLA AGCM coupled to the Geophysical Fluid Dynamics Laboratory (GFDL) Ocean GCM (OGCM) (Ma et al. 1994). The AGCM has a resolution of 4° latitude by 5° longitude, with nine layers in the vertical from the surface to 50 mb. The OGCM (Pacanowski et al. 1991) covers the tropical Pacific basin between 28°S and 50°N, 130°E and 70°W with a resolution of 1° longitude by 0.33° latitude between 10°S and 10°N. Poleward of 10° the meridional grid size increases gradually to 2° at the northern and southern boundaries. The model has 27 levels in the vertical between the surface and the ocean bottom at a constant depth of 4149 m.

The atmospheric planetary boundary layer (PBL) is represented by the lowest model layer in the AGCM, and the PBL depth is a prognostic variable (Suarez et al. 1983). The PBL is assumed to be well mixed. When the PBL top is higher than the condensation level, a stratocumulus cloud layer is assumed to be present between the condensation level and the PBL top. The thickness of the simulated stratocumulus clouds, therefore, can be any fraction of the PBL depth. In addition, the model considers that stratocumulus clouds can be destroyed by instability associated with entrainment into the PBL of air from the free atmosphere and subsequent cooling by the evaporation of cloud liquid water. The criterion for the initiation of this instability is described in Randall (1980). The amount of mixing between air in the PBL and the free atmosphere is determined by requiring that either the cloud layer or unstable conditions disappear, whichever requires less mixing.

The stratus clouds interact with both the shortwave and longwave radiation parameterizations in the AGCM. In the shortwave radiation parameterization (Katayama 1972), stratus clouds are considered to fill the entire grid box, both horizontally and vertically. Low clouds, including stratus clouds, are assumed to be scattering for wavelengths shorter than 0.9 μm, with a reflectivity of 0.66, and absorbing for wavelengths longer than 0.9 μm, with a reflectivity of 0.5 and an absorptivity of 0.3. The longwave radiation parameterization (Harshvardhan et al. 1987) also assumes that clouds fill the grid box vertically but takes into account fractional cloud coverage in the horizontal. The current AGCM relates the fractional cloud coverage to the ratio of the pressure thickness of the stratus to that of the PBL.

We analyze the effect of the stratus clouds off the coast of Peru on the coupled atmosphere–ocean system by performing an idealized experiment in which the amount of stratus clouds is arbitrarily enhanced in selected locations. Specifically, the stratus cover in the AGCM is prescribed over the ocean between 10° and 30°S, and east of 90°W up to the coast of South America (as indicated by the thick lines in Fig. 1). In this region, the stratus amount predicted by the AGCM's parameterization is ignored in both the shortwave and longwave radiation calculations. Instead, it is assumed that stratus clouds are present at all times with a pressure thickness of 30 mb or the PBL depth if it is thinner than 30 mb.

Since observations (e.g., Klein and Hartmann 1993) estimate that the average areal coverage of Peruvian stratus is 40%–70%, this prescription may be unrealistically large for the shortwave radiation. We emphasize that our goal is to assess the sensitivity of the coupled system to the amount of Peruvian stratus rather than to obtain a more realistic simulation with the coupled GCM by prescribing more realistic stratus clouds.

The initial conditions of the experiment with prescribed stratus correspond to 14 July in a long-term coupled GCM integration. The results of this "stratus experiment" are compared to a "control simulation" in which the stratus amount is fully determined by the AGCM. Both model runs cover a common period of 2.5 years. In section 3 we compare results from the last year and consider them indicative of changes in climate and seasonal cycle. In section 4 we concentrate on the initial five months to study the processes involved in the initial adjustments.

3. Impact on climate and seasonal cycle

Figure 3 shows the time evolution of SST averaged over the "Niño-3" equatorial box (2°S–2°N, 150°–100°W) obtained in the control simulation and the stratus experiment. Also shown is the climatological seasonal cycle from observations (Shea et al. 1990). In the control simulation, the Niño-3 SST undergoes quite a realistic seasonal cycle with the cold phase peaking in August and the warm phase in April. In the stratus experiment, which is initialized in July, the seasonal warming is replaced by an initial cooling through the following January. The subsequent two years exhibit seasonal cycles that resemble each other. Compared to

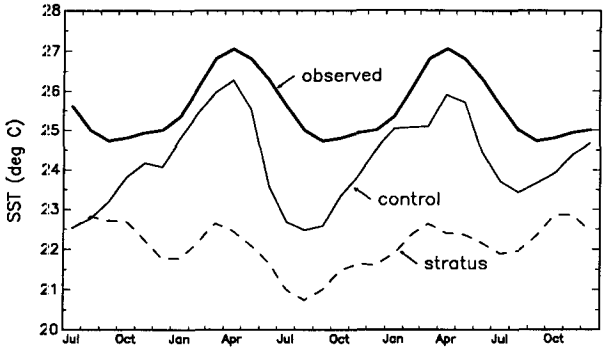

FIG. 3. SST over the Niño-3 region (2°S–2°N, 150°–100°W) for the control simulation (solid line), the stratus experiment (dashed line), and the observed climatological seasonal cycle (thick solid line).

the control simulation, the Niño-3 SST of the stratus experiment is significantly lower and has a seasonal cycle with a similar timing but a much reduced amplitude that is too weak compared to observations. The small amplitude may be partly due to the lack of seasonal dependence of the prescribed stratus.

To examine the changes in climate and seasonal cycle across the basin, the last year of the integration is taken as representative. Interannual variability in the control simulation (cf. Robertson et al. 1995a) is much smaller in amplitude than the features to be described below, while the initial adjustment to the prescribed stratus appears to be confined within the first few months.

The enhanced Peruvian stratus has a clearly visible impact on the horizontal distributions of SST, surface wind stress, and precipitation shown for April and October in Figs. 4–6. Corresponding observational estimates are also shown, with the SST distributions from Shea et al. (1990) and the wind stress and precipitation distributions from da Silva et al. (1994). In both months the region of prescribed stratus shows a large decrease in SST (Fig. 4). A noticeable decrease in SST also extends across the southeastern Pacific into a broad equatorial band. The systematic warm bias of the coupled GCM off the Peruvian coastal region is alleviated, although over the eastern Pacific along 5°S a tongue of relatively warm SSTs with respect to the north and south persists in the stratus experiment. On the other hand, the model's extensive cold bias along the equator and throughout most of the southern subtropics is exacerbated in the stratus experiment.

At the equator, the SST in the stratus experiment shows an unrealistically strong and persistent cold tongue that extends right across the basin. This feature, which is especially unrealistic in April when the cold tongue is practically absent in observations, accounts for the small amplitude of the seasonal cycle of SST as seen in the Niño-3 SST (Fig. 3). Despite the lack of seasonal variation, the stratus experiment does exhibit a more realistic zonal contrast in SST south of the equator in both April and October, with the warm pool better localized in the western Pacific, albeit bisected by the overly strong cold tongue at the equator.

Compared to the control simulation, the stratus experiment produces stronger and more realistic southeast trades (Fig. 5). In April, in particular, the zonal wind stress at the equator is much stronger in the stratus experiment, consistent with the effects of larger zonal thermal gradients on the one hand and its effect on equatorial upwelling through enhanced Ekman pumping on the other. A serious deficiency in the control simulation in April is the penetration of the northeast trades south of the equator, associated with the ITCZ crossing the equator (Robertson et al. 1995b). In the stratus experiment this deficiency is corrected, and a more realistic distribution of the northeast trades is obtained. Farther westward, however, the southeast trades are obtained. In both April and October, the cross-equatorial flow near the eastern end of the basin is significantly improved in the stratus experiment, consistent with the larger north–south SST contrast. Farther westward, however, the southeast trades still tend to weaken unrealistically right at the equator.

The corresponding distributions of precipitation (Fig. 6) are important indicators of the convergence zones and diabatic heat sources that drive the atmospheric circulation. In April, the precipitation maximum in the eastern Pacific is unrealistically displaced south of the equator in the control simulation. This situation is greatly improved in the stratus experiment, which produces a much more realistic South Pacific convergence zone (SPCZ). Similarly in October, the SPCZ is better simulated with the precipitation maximum confined in the western Pacific. All these changes are consistent with the effects of colder SSTs in the stratus experiment on convection in the southeastern Pacific and the improved low-level winds in the stratus experiment.

In summary, the prescribed stratus clouds over the southeastern Pacific has the effect of alleviating the warm SST bias local to the stratus region while further decreasing SSTs that are already too cold in the coupled GCM. They also cause the equatorial cold tongue to persist throughout the year, thus greatly diminishing the amplitude of the seasonal cycle in equatorial SST. Although the seasonal variation of equatorial SST in the control simulation is overestimated, that in the stratus experiment is too weak compared to observations. This can be partly attributed to the lack of seasonal variation in the prescribed stratus deck. From the point of view of surface wind stress and precipitation, however, the annual mean climate is greatly improved by the prescribed stratus deck: equatorial wind stress values are increased to realistic values, the ITCZ remains north of the equator, and the SPCZ is much better localized.

4. Analysis of initial adjustment

To gain insight into the physical processes associated with the large sensitivity of the coupled GCM to Peru-

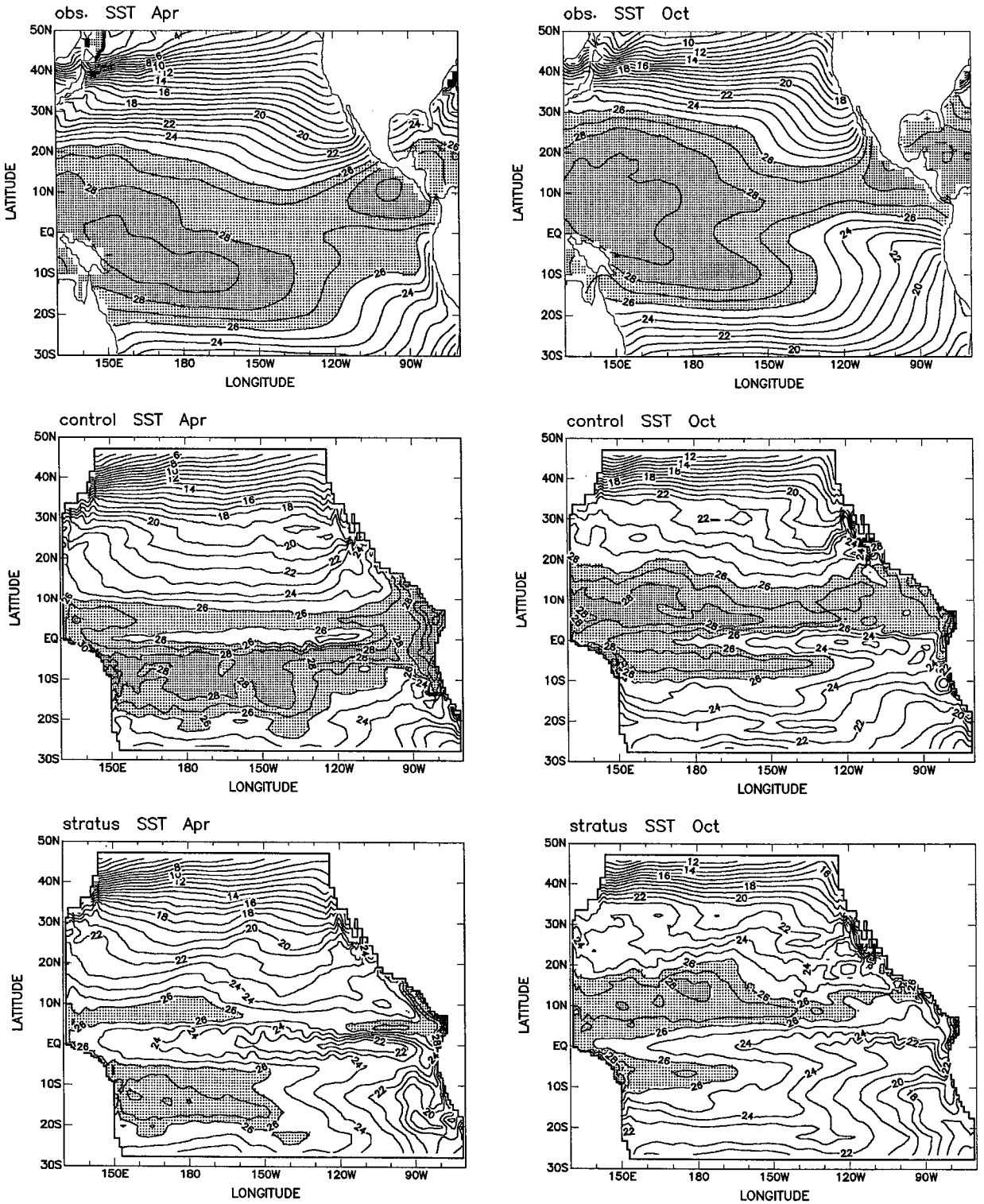

FIG. 4. Sea surface temperature (°C) in April (left panels) and October (right panels) of observations (upper panels), the control simulation (middle panels), and the stratus experiment (lower panels).

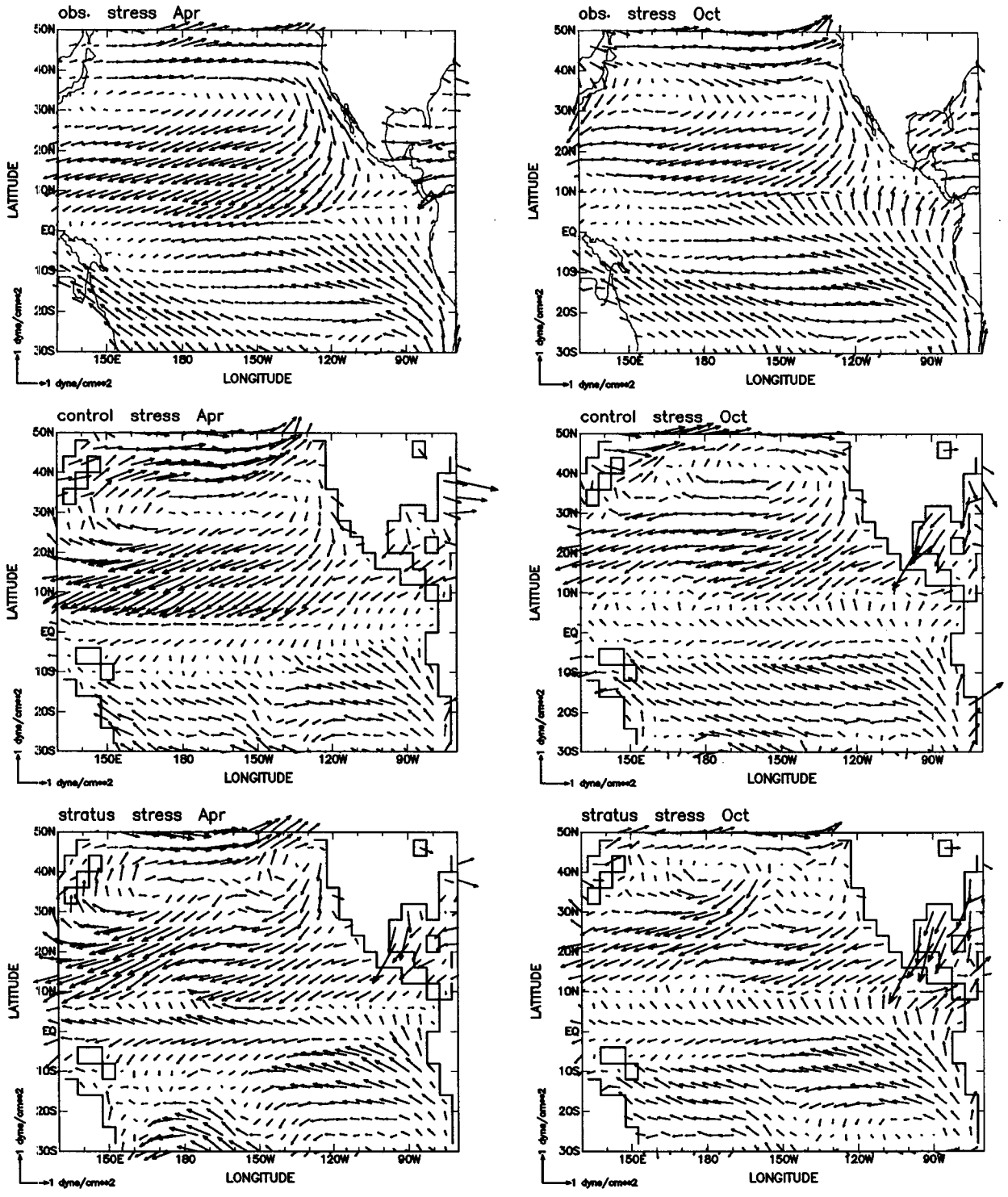

FIG. 5. Surface wind stress in April (left panels) and October (right panels) of observations (upper panels), the control simulation (middle panels), and the stratus experiment (lower panels). These maps encompass the domain of the ocean model.

vian stratus, we examine the thermodynamic evolution of the ocean surface layer during the initial five months of the two integrations that start from the same initial condition. Figure 7 shows the SST differences between the stratus experiment and the control simulation in October and December—three and five months into the

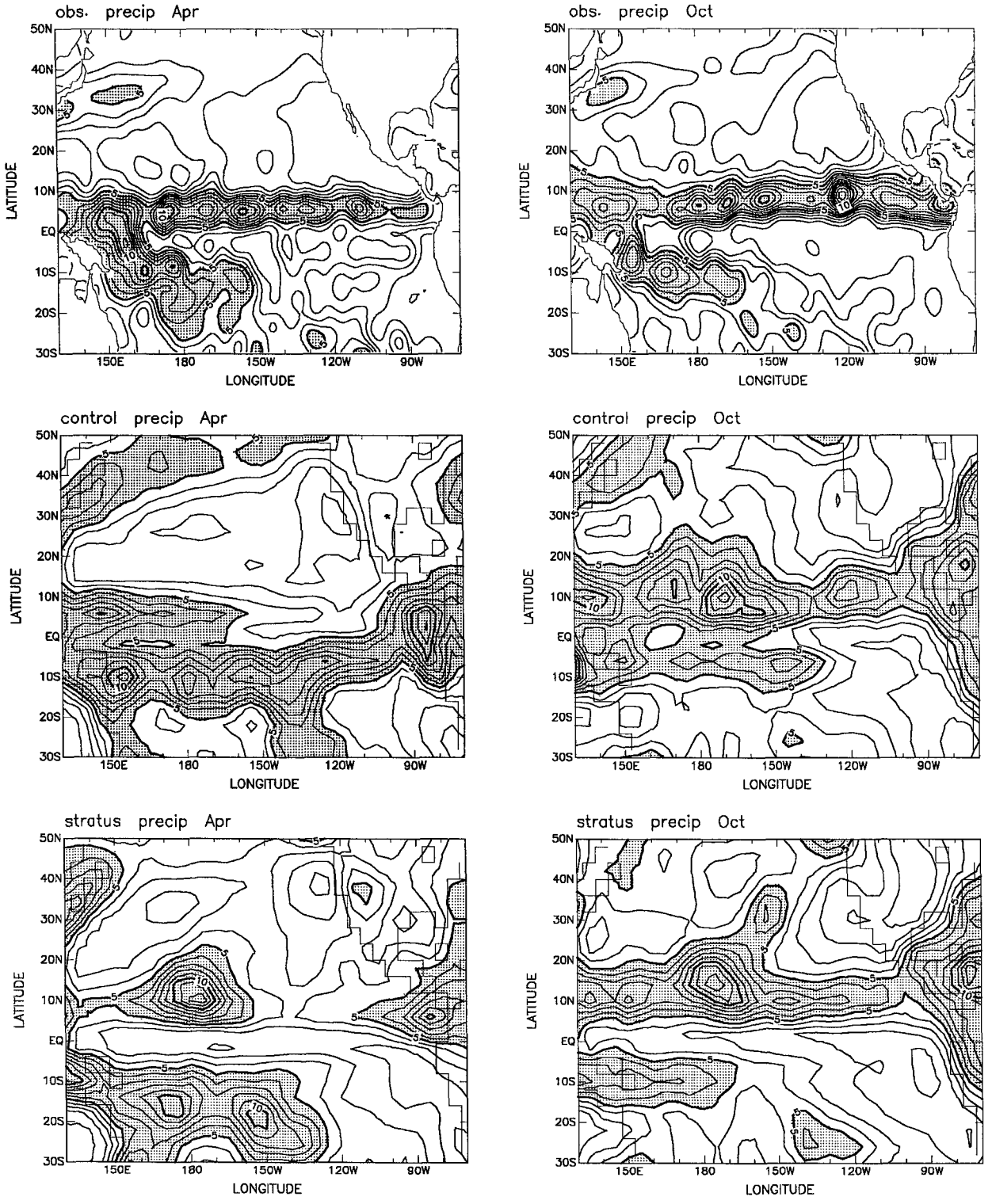

FIG. 6. Precipitation (mm d^{-1}) in April (left panels) and October (right panels) of observations (upper panels), the control simulation (middle panels), and the stratus experiment (lower panels). These maps encompass the domain of the ocean model. Contour interval is 1 mm d^{-1}; regions with values larger than 5 mm d^{-1} are stippled.

model integrations, respectively. By October, there is a strong cooling inside and to the north of the region where the stratus clouds are prescribed. The strongest cooling by up to 5 K occurs around 10°S, where the thermocline is shallow. Between October and December, the region of cooling extends westward rapidly, especially within the equatorial belt between 8°S and 8°N. This evolution is accompanied by an enhancement of the southeast trades over the eastern Pacific Ocean.

The SST cooling in the region where stratus clouds are prescribed results from reduced solar radiation reaching the surface, which is only partially offset by increased downward longwave emission by the stratus. On the average, the increase in stratus cover decreases the surface shortwave radiation by 100–150 W m^{-2}, depending on the season, and decreases the net upward longwave radiation at the surface by 70–90 W m^{-2}.

To identify the dominant processes involved in the cooling at locations away from the prescribed stratus region, we analyze the relative importance of terms in the temperature equation of the uppermost layer of the OGCM:

$$\frac{\partial T}{\partial t} = -\mathbf{v}\cdot\nabla T - w\frac{\partial T}{\partial z} + \frac{1}{\rho c_p}\frac{\partial H}{\partial z} + \frac{\partial}{\partial z}\left(K_H\frac{\partial T}{\partial z}\right). \quad (1)$$

Here T is potential temperature, t is time, $\mathbf{v}$ is horizontal velocity, ∇ is the horizontal gradient operator, w is vertical velocity, z is the vertical coordinate, H is vertical heat flux, ρ is density, and c_p is the specific heat of water. The value of the vertical diffusion coefficient, K_H, is determined by the Mellor–Yamada level $2\frac{1}{2}$ turbulence closure scheme (Mellor and Yamada 1982). The terms on the right-hand side of (1) represent the horizontal advection, vertical advection, heating by surface heat flux, and turbulent vertical diffusion, respectively. In fact, the temperature in the OGCM can also change due to horizontal diffusion and convective adjustment. The effect of horizontal diffusion is expected to be small. Temperature changes due to convective adjustments are not part of the standard archive of the OGCM. These two processes, therefore, are not included in the analysis, and the relative importance of their combined contribution will be discussed with the results of the analysis.

Averaging (1) vertically over the uppermost layer of the OGCM (from $-\Delta z = -10$ m to the surface $z = 0$), we obtain

$$\frac{\partial T_1}{\partial t} = -\mathbf{v}_1\cdot\nabla T_1 - \frac{1}{2}w_{-\Delta z}\frac{T_1 - T_2}{\Delta z} + \frac{1}{\Delta z}\frac{H_s}{\rho c_p} - \frac{1}{\Delta z}\left(K_H\frac{\partial T}{\partial z}\right)\Bigg|_{-\Delta z}, \quad (2)$$

where subscripts 1, s, and $-\Delta z$ denote values at the first level, surface, and the interface between the first and second levels, respectively. In the simulations performed for this study the solar radiation does not penetrate into the deeper ocean layers. The entire surface heat flux H_s, therefore, is absorbed by the first layer.

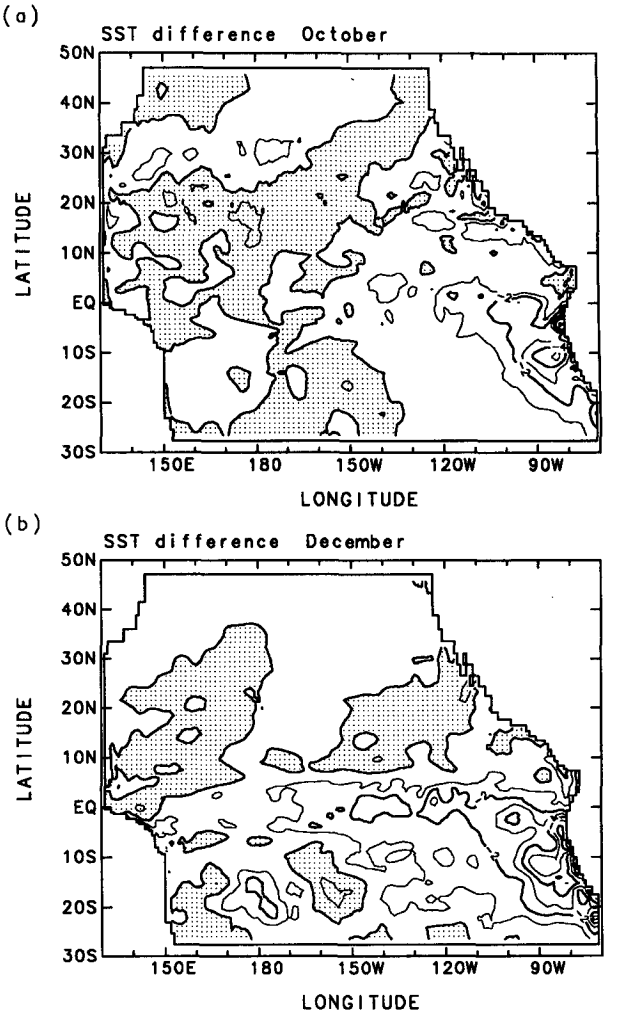

FIG. 7. Difference in simulated SST between the stratus experiment and the control simulation for (a) October and (b) December. Contour interval is 1 K; regions with positive values are stippled.

Each term on the right-hand side of (2) is obtained using model-archived 3-day means. The advective terms are computed from 3-day means of horizontal and vertical velocities and temperature, while 3-day means of the surface heat flux H_s and vertical diffusive flux $K_H\partial T/\partial z$ are directly archived by the OGCM. We then take the difference of each term between the two experiments and compute the corresponding time integrals to measure the accumulated effect of each term on the SST difference. In this way, fluctuations due to short-term transients are filtered out. The sum of these time-integrated differences—which we will call the diagnosed SST difference—can be compared against the actual SST difference from the two simulations and thus provides a measure of the size of the neglected

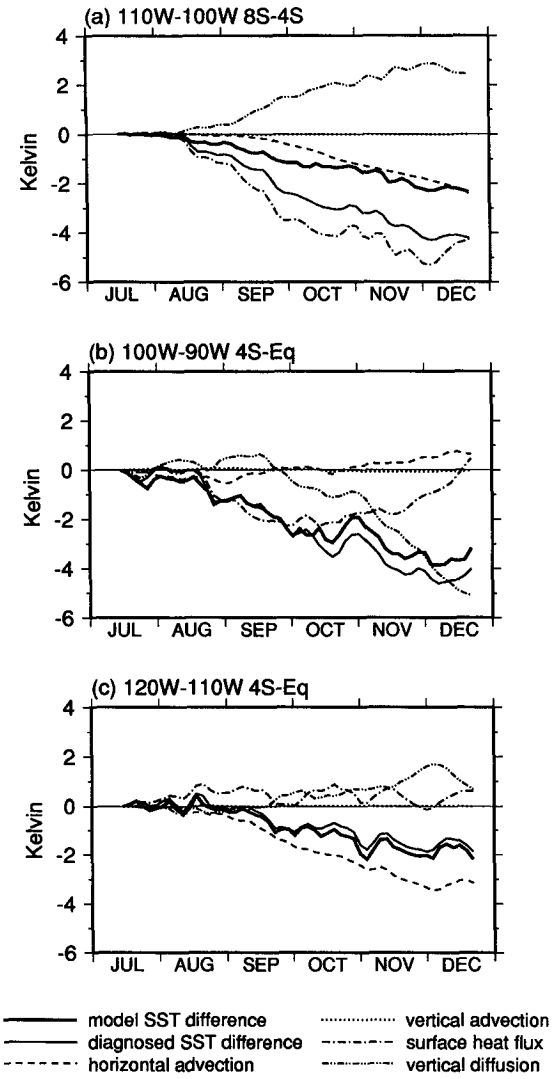

FIG. 8. Time-integrated SST difference between the stratus experiment and the control simulation due to horizontal advection (dashed), vertical advection (dotted), surface heat flux (dash–dot), vertical diffusive flux (dash–dot–dot), and their sum (solid) for (a) 8°–4°S, 110°–100°W; (b) 4°S–equator, 100°–90°W; and (c) 4°S–equator, 120°–110°W. Thick solid line shows the difference in SST actually simulated by the coupled GCM.

terms and errors arising from computing the advection terms from 3-day means.

The analysis described above is performed at each grid point and then spatially averaged over 10° longitude by 4° latitude boxes. Examination of the contributions from each term reveals three distinct types of evolution, typified by the three boxes shown in Fig. 8. South of 4°S, changes in the surface heat flux account for most of the cooling in the stratus experiment relative to the control simulation, with horizontal advection playing a minor role between 8°S and 4°S east of 110°W (Fig. 8a). The vertical diffusion has a strong compensating effect on the surface cooling, indicative of a downward mixing of the surface cooling. In the equatorial band (4°S–4°N) east of 110°W both surface heat flux and vertical diffusion are important (Fig. 8b), while west of 110°W the horizontal advection is the dominant process (Fig. 8c).

Figure 9 summarizes the geographical distribution of the dominating process for the SST difference between the stratus experiment and the control simulation. In the eastern part of the basin away from the equator, the difference in surface heat flux plays the dominant role. Further analysis shows that this is largely due to greater evaporative cooling, which is primarily associated with larger surface wind speed in the stratus experiment. This indicates that it is primarily changes in atmospheric circulation that cause SST changes in these regions and explains the rapid establishment of the differences between the two integrations. Ocean advection becomes dominant only near the equator and west of 110°W; it is responsible for the cooling in the central equatorial Pacific. The situation is more complex in the eastern equatorial region, where the vertical diffusive flux plays a nonnegligible role. In this region the mixed layer is shallow, and vertical mixing can be easily influenced by changes in the surface wind.

In general, the overall trend and variation in the SST difference between the two experiments are accounted for by the terms considered in (1). The disagreement between the diagnosed and simulated SST differences reflects the effects of convective adjustment and horizontal diffusion together with the accumulation of errors with time. The closest agreements are obtained in boxes on the south side of the equator (4°S–equator) where the two differ by less than 1 K over five months. In regions equator–4°N and 8°–4°S the discrepancies

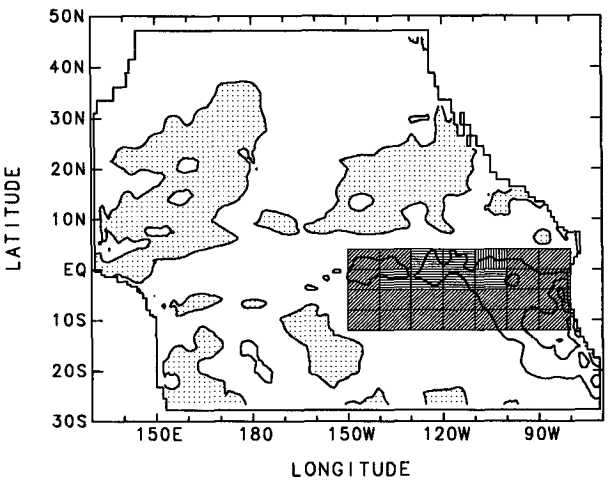

FIG. 9. A figure showing the dominant term in the temperature equation that contributes to the difference in SST between the stratus experiment and the control simulation in various regions. Horizontal hatching indicates where horizontal advection dominates, vertical hatching indicates vertical diffusion, and diagonal hatching indicates surface heat flux. Also shown is the SST difference in December with 2-K contour interval.

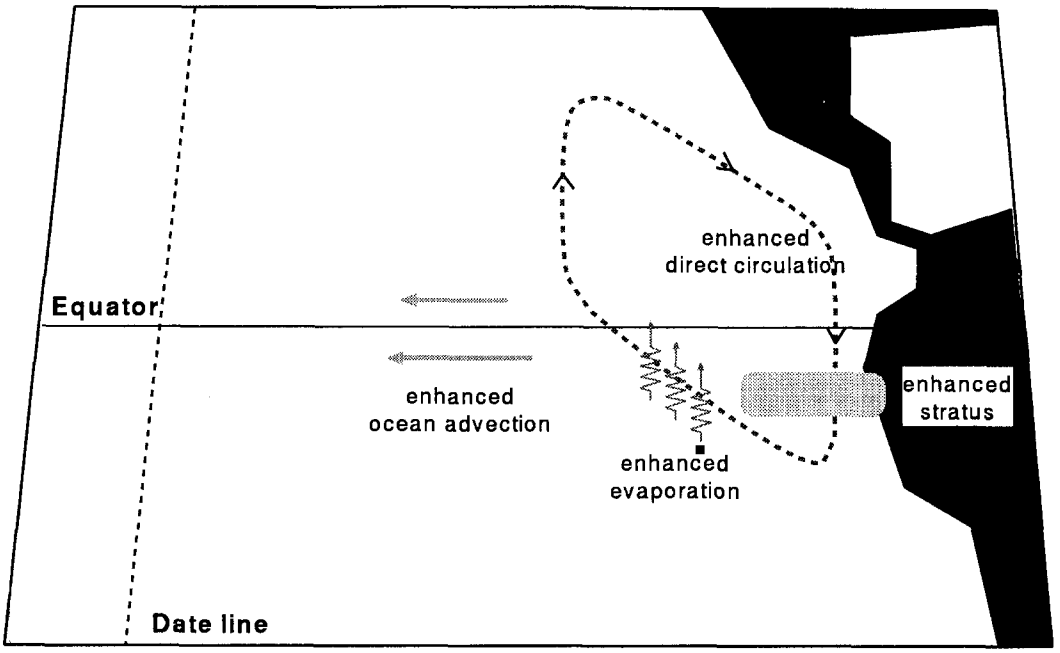

FIG. 10. A schematic illustrating the influence of Peruvian stratus on tropical atmospheric and oceanic circulations as suggested by the coupled GCM experiment.

are larger but still within 3 K. The discrepancies are largest south of 8°S. In this region there is strong surface cooling due to changes in radiation at the surface in the stratus experiment and convective adjustment is likely to be more active. The overestimated cooling is consistent with neglecting the compensating warming effect of convective adjustments on the surface layer. Although this effect appears to be quite significant south of 4°S, the surface heat flux term is clearly the dominant term.

5. Conclusions

In this paper we investigate the influence of Peruvian stratus clouds on the tropical circulation. A coupled GCM simulation is performed in which a large amount of stratus is prescribed in a region off the coast of Peru, where the coupled GCM underestimates the incidence of stratus clouds. The coupled model simulation shows great sensitivity to the amount of Peruvian stratus. The results and implications of this study can be summarized as follows.

1) The increase in stratus cloud amount in the southeastern Pacific, by reducing shortwave radiation reaching the surface, can lower the SST by up to 5 K. This cooling is sufficient to account for the warm bias in this region in the coupled simulations (Fig. 1). The decrease in SST also results in stronger and more realistic asymmetries—both north–south and east–west—in SST distribution. The surface wind stress and precipitation distributions also improve substantially. While the model's annual mean climatology is significantly improved in terms of overall pattern and strength of the low-level winds, the cold bias in SST along the equator is exacerbated, with a strong cold tongue persisting throughout the year.

2) The Peruvian stratus clouds exert a strong influence on the climate in regions away from the coast of Peru.[1] A substantial cooling even extends westward along the equator to the date line. Different mechanisms are responsible for the remote effect in different regions as shown schematically in Fig. 10. The enhanced large-scale meridional and zonal SST gradients drive a thermally direct circulation that strengthens the Walker–Hadley circulation. These changes in atmospheric circulation increase the surface wind speeds and thereby enhance evaporation over the eastern Pacific. This increased evaporation accounts for the cooling of SST in the proximity of the prescribed stratus region. At the equator, enhanced oceanic cold advection is largely responsible for the stronger cold tongue in the stratus experiment away from the coast.

3) The lower SSTs obtained by increasing stratus off the coast of Peru do not seem to eradicate the coupled GCM's tendency to produce a zonally oriented belt of warm SSTs south of the equatorial cold tongue. Despite the sizeable prescribed stratus deck, there is still a region of relatively high SST near 5°S in the

[1] After this manuscript was prepared, the authors became aware that a similar result was obtained by the Meteorological Research Institute, Japan (Tokioka 1995, personal communication).

stratus experiment. Precipitation in this region is greatly reduced to realistic levels, but there is still an unrealistic surface wind convergence.

The analysis in this paper employed a single 2-yr anomaly-control pair of coupled GCM simulations initialized during the peak phase of the seasonal equatorial cold tongue in the control integration. The transition phase may be sensitive to the phase of the seasonal cycle of the initial condition. It may also be influenced by intraseasonal timescale variability both in the model ocean and atmosphere. In view of these considerations, we performed a second stratus experiment that was initialized in July of a different year of the long-term coupled simulation. The major features found in the first experiment, including the nonlocal cooling, were also obtained in the second experiment despite differences in the details of the evolutions.

Philander et al. (1996a) found that the feedback provided by stratus clouds—low SST promotes the formation of stratus clouds which tend to further decrease the SST—is crucial in producing realistic meridional asymmetries in the eastern Pacific. By introducing an empirical formulation of reduction of surface shortwave radiation by stratus clouds in their coupled GCM, they obtained significant cooling in the SST throughout the tropical Pacific, especially over southeastern Pacific. They also noted excessively low SSTs along the equator. Despite the differences in model components and the manner stratus clouds are introduced, their findings and ours share similarities in the role of stratus clouds on tropical circulation.

The results of this study strongly support the contention that coupled GCM simulations can benefit substantially from improved parameterization of the marine stratus clouds. In the UCLA AGCM, the deficiencies in the simulation of stratus clouds may be due to several factors: 1) the layer cloud instability parameterization may be too efficient in destroying stratus clouds, 2) the rather coarse horizontal resolution in the current AGCM may introduce fictitious influence of land over coastal regions through the horizontal advection of drier air, 3) the vertical moisture transport across the PBL top may be overestimated. On the other hand, the results also indicate that deficiencies in simulated stratus clouds are not the sole cause of the systematic errors in current coupled GCM simulations. Other aspects of the model components also deserve attention.

Acknowledgments. The authors would like to thank Mr. Joseph Spahr for his assistance with the UCLA AGCM. This work was supported by DOE-CHAMMP under Grant DE-FG03-91ER61214 (CCM, CRM, AA), by NOAA under Grant NA56GP0222 (CRM, AA), by ONR under Grant N00014-93-1-0673 (CCM), and by NOAA under Grant NA46GP0244 (AWR). Model integrations were performed at the San Diego Supercomputer Center.

REFERENCES

Bjerknes, J., 1969: Atmospheric teleconnections from the equatorial Pacific. *Mon. Wea. Rev.*, **97,** 163–172.

da Silva, A. M., C. C. Young, and S. Levitus, 1994: *Atlas of Surface Marine Data 1994. Volume 1: Algorithms and Procedures.* National Oceanic and Atmospheric Administration, 83 pp.

Dijkstra, H. A., and J. D. Neelin, 1995: Ocean–atmosphere interaction and the tropical climatology. Part II: Why the Pacific cold tongue is in the east. *J. Climate,* **8,** 1343–1359.

Giese, B. S., and J. A. Carton, 1994: The seasonal cycle in a coupled ocean–atmosphere model. *J. Climate,* **7,** 1208–1217.

Harshvardhan, R. Davies, D. A. Randall, and T. G. Corsetti, 1987: A fast radiation parameterization for atmospheric circulation models. *J. Geophys. Res.*, **92,** 1009–1016.

Jin, F.-F., J. D. Neelin, and M. Ghil, 1994: El Niño on the devil's staircase: Annual subharmonic steps to chaos. *Science,* **264,** 70–72.

Katayama, A., 1972: A simplified scheme for computing radiative transfer in the troposphere. Tech. Rep. 6, University of California, Los Angeles, 77 pp.

Klein, S. A., and D. L. Hartmann, 1993: The seasonal cycle of low stratiform clouds. *J. Climate,* **6,** 1587–1606.

Ma, C.-C., C. R. Mechoso, A. Arakawa, and J. D. Farrara, 1994: Sensitivity of a coupled ocean–atmosphere model to physical parameterizations. *J. Climate,* **7,** 1883–1896.

Mechoso, C. R., A. W. Robertson, N. Barth, M. K. Davey, P. Delecluse, P. R. Gent, S. Ineson, B. Kirtman, M. Latif, H. Le Treut, T. Nagai, J. D. Neelin, S. G. H. Philander, J. Polcher, P. S. Schopf, T. Stockdale, M. J. Suarez, L. Terray, O. Thual, and J. J. Tribbia, 1995: The seasonal cycle over the tropical Pacific in coupled ocean–atmosphere general circulation models. *Mon. Wea. Rev.,* **123,** 2825–2838.

Mellor, G. L., and T. Yamada, 1982: Development of a turbulence closure model for geophysical fluid problems. *Rev. Geophys. Space Physics,* **20,** 851–875.

Pacanowski, R. C., K. Dixon, and A. Rosati, 1991: The GFDL modular ocean model user guide. Tech. Rep. 2, GFDL Ocean Group.

Philander, S. G. H., D. Gu, D. Halpern, G. Lambert, N.-C. Lau, T. Li, and R. C. Pacanowski, 1996a: The role of low-level stratus clouds in keeping the ITCZ mostly north of the equator. *J. Climate,* **9,** in press.

——, T. Li, G. Lambert, and R. C. Pacanowski, 1996b: Climate asymmetries relative to the equator. *Nature,* submitted.

Randall, D. A., 1980: Conditional instability of the first kind upside-down. *J. Atmos. Sci.,* **37,** 125–130.

Robertson, A. W., C.-C. Ma, M. Ghil, and C. R. Mechoso, 1995a: Simulation of the tropical Pacific climate with a coupled ocean–atmosphere general circulation model. Part II: Interannual variability. *J. Climate,* **8,** 1199–1216.

——, ——, C. R. Mechoso, and M. Ghil, 1995b: Simulation of the tropical Pacific climate with a coupled ocean–atmosphere general circulation model. Part I: The seasonal cycle. *J. Climate,* **8,** 1178–1198.

Shea, D. J., K. E. Trenberth, and R. W. Reynolds, 1990: A global monthly sea surface temperature climatology. Tech. Note TN-345+STR, NCAR, Boulder, CO, 167 pp.

Stockdale, T., M. Latif, G. Burgers, and J.-O. Wolff, 1994: Some sensitivities of a coupled ocean–atmosphere GCM. *Tellus,* **46A,** 367–380.

Suarez, M. J., A. Arakawa, and D. A. Randall, 1983: The parameterization of the planetary boundary layer in the UCLA general circulation model: Formulation and results. *Mon. Wea. Rev.,* **111,** 2224–2243.

Xie, S.-P., 1994: The maintenance of an equatorially asymmetric state in a hybrid coupled GCM. *J. Atmos. Sci.,* **51,** 2602–2612.

——, and S. G. H. Philander, 1994: A coupled ocean–atmosphere model of relevance to the ITCZ in the eastern Pacific. *Tellus,* **46A,** 340–350.